MASTER

Segregation processes in small bimetallic clusters on supported catalysts studied by LEIS

Nooij, O.W.

Award date:
1998

Segregation processes in small bimetallic clusters on supported catalysts studied by LEIS.

O.W. Nooij May 1995

Master Thesis

Eindhoven University of Technology
Department of Physics

and

Schuit Institute of Catalysis

Co workers :

H.H. Brongersma
A.W. Denier van der Gon
L.C.A van den Oetelaar
A.G. Roosenbrand
J.A.R. van Veen

Summary.

In this work it will be shown that, with the new developed ERISS apparatus, Static Low Energy Ion Scattering (SLEIS) experiments can be performed on fragile surfaces like supported metal catalysts.

The surface composition of Pd-Pt clusters (~ 5nm), with different Pt/Pd ratios (4/1 and 1/4), on a γ-Al_2O_3 support is studied by LEIS. To determine and quantify the segregation processes in the supported clusters, a comparison is made with bulk alloys with the same composition. Reduction of the catalysts in 500 mbar H_2 at 350°C results in a 100% Pt enrichment on the catalyst clusters of both compositions. This, contrary to the Pd enrichment on the surface of the alloys. This is explained by a model where H_2 adsorbs dissociatively on the clusters and migrates to the cluster/support interface and causes a (partial) reduction of the support at the interface and subsequently Al-alloys are formed at the interface. Changes in the interface energy causes the cluster to break up or to spread through wetting.

Table of contents

1. Introduction.

To enhance chemical reaction rates selectively, catalysts are widely used in industry. Several kinds of catalysts can be distinguished. In heterogeneous catalysis the separation of reactants/products (often gas phase) and catalyst (often solid) is easy because they exist in different phases, this in contrast to homogeneous catalysis. Heterogeneous catalysts are used in many different forms like the solid acids, mixed metal oxides and supported metal catalysts. Bimetallic catalysts are a subgroup of the last, where bimetallic clusters are present at the surface of a highly porous support. The pores in the support provide a large surface area in the order of several hundred square meters per gram support material. Typical materials used as support are alumina, silica, zeolites and carbon. Reactions take place on the surface of the small metal clusters and therefore the catalytic selectivity will strongly depend on the surface composition of the bimetallic clusters [1]. The surface composition can also determine important properties such as the resistivity of the catalyst against poisoning by for example sulphur [2]. Therefore it is important to know the surface composition of these clusters and the processes that influence the surface composition. Consequently, experimental studies in which the outermost layer of small bimetallic clusters is probed are necessary to get a better understanding of the segregation processes, which influence the surface composition.

Segregation processes in bimetallic systems as alloys and supported bimetallic clusters can be induced by several parameters. Parameters that play a role in the segregation processes in bulk alloys are:
Surface free energies of the metals, the compound with the lowest surface free energy will tend to segregate to the surface; the atomic size of the compounds; the heat of solution, important for compound formation; the temperature which determines the mobility of the atoms; the presence of adsorbates can cause chemical induced segregation.
For supported bimetallic clusters also two other aspects play a role in the segregation processes : the cluster size, this means a limited supply of atoms and a relatively large part of the atoms are surface atoms; the interface energy, as with the surface free energies, the compound with the lower interface energy will tend to segregate to the interface.

A great variety of techniques is available to study the surfaces of solid materials. Many of these techniques are not suited for the study of industrial catalysts because they require flat surfaces or even single crystals, e.g. Atomic Force Microscopy (AFM) and Low Energy Electron Diffraction (LEED). Others can not be used because they can not handle insulating samples, e.g. Secondary ion mass spectroscopy (SIMS) and Auger Electron

Spectroscopy (AES). X-ray Photoelectron Spectroscopy (XPS) and AES are commonly used in studies of industrial catalysts. Recently A.G. Sault [3] has shown that for XPS, with attenuation lengths in the order of 1-2 nm, it is often not possible to detect preferential surface enrichment of one of the metals in bimetallic clusters for cluster sizes below 8 nm. In ideal cases where complete segregation occurs, detection may be possible for clusters as small as 3 nm, although these results should be viewed with suspicion.

Low Energy Ion Scattering (LEIS) is a technique capable of probing the outermost surface layer [5]. In LEIS noble gas ions with a known energy of several keV, are scattered elastically in a binary collision at the surface. The energy of the scattered ion depends on the initial energy of the ion, the scattering angle and the mass of the atom from which it scattered. When the scattering angle is fixed, the mass of the surface atom can be calculated from the energy of the scattered ion. Noble gas ions scattered from deeper surface layers will be neutralized because of the high neutralization probability and since in the experiment only ions are detected, the LEIS signal represents only the ions scattered from the outermost surface layer of the solid. A disadvantage of detecting only the outermost surface layer is the significant influence of adsorbates or contaminants on the detected LEIS signals.

Due to sputter damage to the surface by the incident ions and the high ion doses needed, LEIS was not used for studies on small supported bimetallic clusters. The ion doses needed to obtain reasonable spectra with for instance a cylindrical mirror analyzer can cause too much damage to fragile surfaces like supported metal catalysts. With the newly developed ERISS apparatus [4] ion doses can be reduced to such a low level that static LEIS is obtained, i.e. the surface has only negligible damage, not more than a few percent of the surface atoms are part of a scattering event.

In this work we will first demonstrate that the ERISS apparatus can indeed perform static LEIS measurements on supported metal catalyst. As an illustration of the possibilities of the technique we will then proceed with a study of segregation processes in small bimetallic clusters of platinum and palladium on an alumina substrate. The catalysts consists of an Al_2O_3 support with a specific area of 200 m^2/g and is loaded with 1 wt% platinum and palladium in small bimetallic clusters of on average 5 nm in diameter. Two different bulk concentrations of platinum and palladium were used, one with 80 at% Pt and 20 at% Pd the other with 20 at% Pt and 80 at% Pd. The catalysts are produced at the Koninklijke/Shell Laboratory in Amsterdam (KSLA). To make a comparison with bulk alloys, two alloys with the same Pt/Pd ratio as the catalysts were also studied. These alloys were produced by the Philips NatLab. For calibration purposes pure Pt and Pd samples were used.

2. Method.

The final energy E_f of a scattered particle with a kinetic energy E_i and mass M_1 and a particle at rest, i.e. a binary collision, can be calculated from conservation of energy and momentum. This final energy depends besides E_i and M_1 only on the mass of the particle initially at rest, M_2, and the scattering angle Θ. By fixing E_i, M_1 and Θ, the energy spectrum of E_f corresponds to a mass spectrum of the surface. A typical LEIS spectrum of a Pd-Pt alloy is shown in figure 2.1. For this measurement a 3keV Ne^+ beam was used with a current of 200 pA. The manipulator was scanned under the ion beam over an area of 0.11 cm^2. With a measurement time of 70 seconds this results in an extremely low ion dose of $8 \cdot 10^{11}$ ions/cm^2. In the spectrum shown, the horizontal axis indicates the energy of the ions after scattering, the vertical axis shows the number of detected scattered ions at every energy interval. In the spectrum two surface peaks are clearly distinctive. One corresponds to the palladium on the surface and the other to the platinum on the surface.

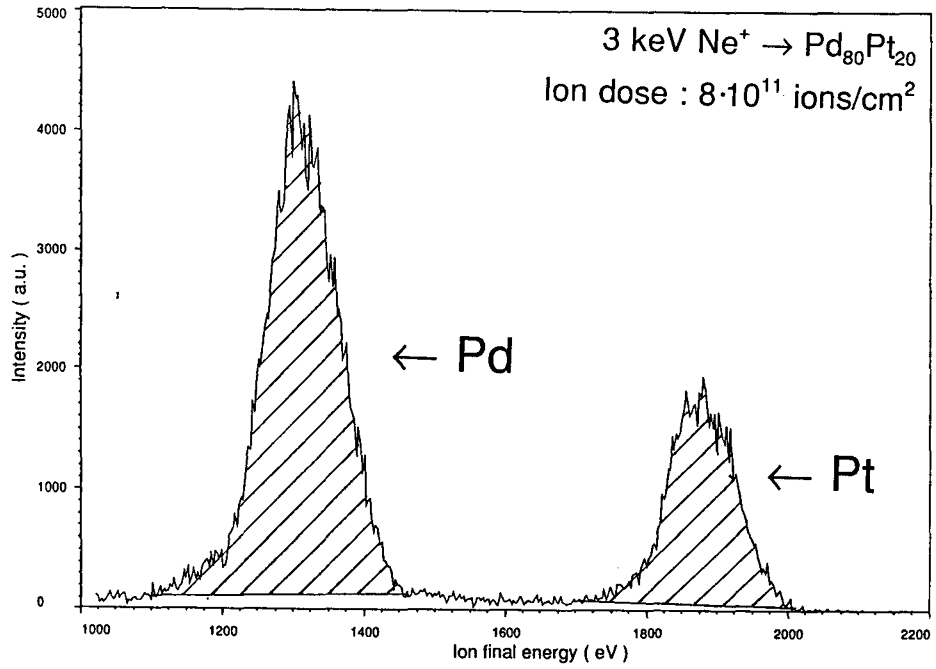

***Figure 2.1** Typical LEIS spectrum of a $Pd_{80}Pt_{20}$ alloy taken with an ion beam of 3keV Ne^+ ions and an ion dose of $8 \cdot 10^{11}$ ions/cm^2.*

The area under the peak is a measure for the amount of the corresponding element on the surface. In the following the area under a peak will be denoted as S. As will be explained in the next paragraph the concentration of atoms can be determined by comparing the area under a peak with the area under a peak obtained from a pure sample, i.e. through calibration against pure metals.

To obtain surface sensitivity noble gas ions are used. Due to their very high neutralization probability, effectively only ions scattered at the outermost surface will have a reasonable chance of not being neutralized. The total signal from element i (S_i) is related to the concentration of element i (c^s_i) at the surface :

$$S_i = I_t \cdot (d\sigma/d\Omega)_i \cdot P^+_i \cdot \varepsilon \cdot c^s_i$$

where I_t is the incident ion fluence, $(d\sigma/d\Omega)_i$ the differential scattering cross section of element i, P^+_i the ion survival probability, ε an experimental constant and c^s_i the surface concentration. P^+_i can not be calculated, therefore quantification in LEIS is done by using pure elements as calibration samples :

$$c^s_i = c^s_c \, (S_i/S_c)$$

where c^s_c is the known surface concentration of the pure element and S_c and S_i the measured intensity of the calibration sample and the sample under investigation respectively. This calibration method is not valid if so-called "matrix-effects" occur, i.e. if the ion survival probability depends on the chemical environment of the element; $P^+_i \neq P^+_c$. For platinum and palladium no "matrix-effects" were found in previous studies **[18]**.

3. Experimental.

3.1 Experimental setup.

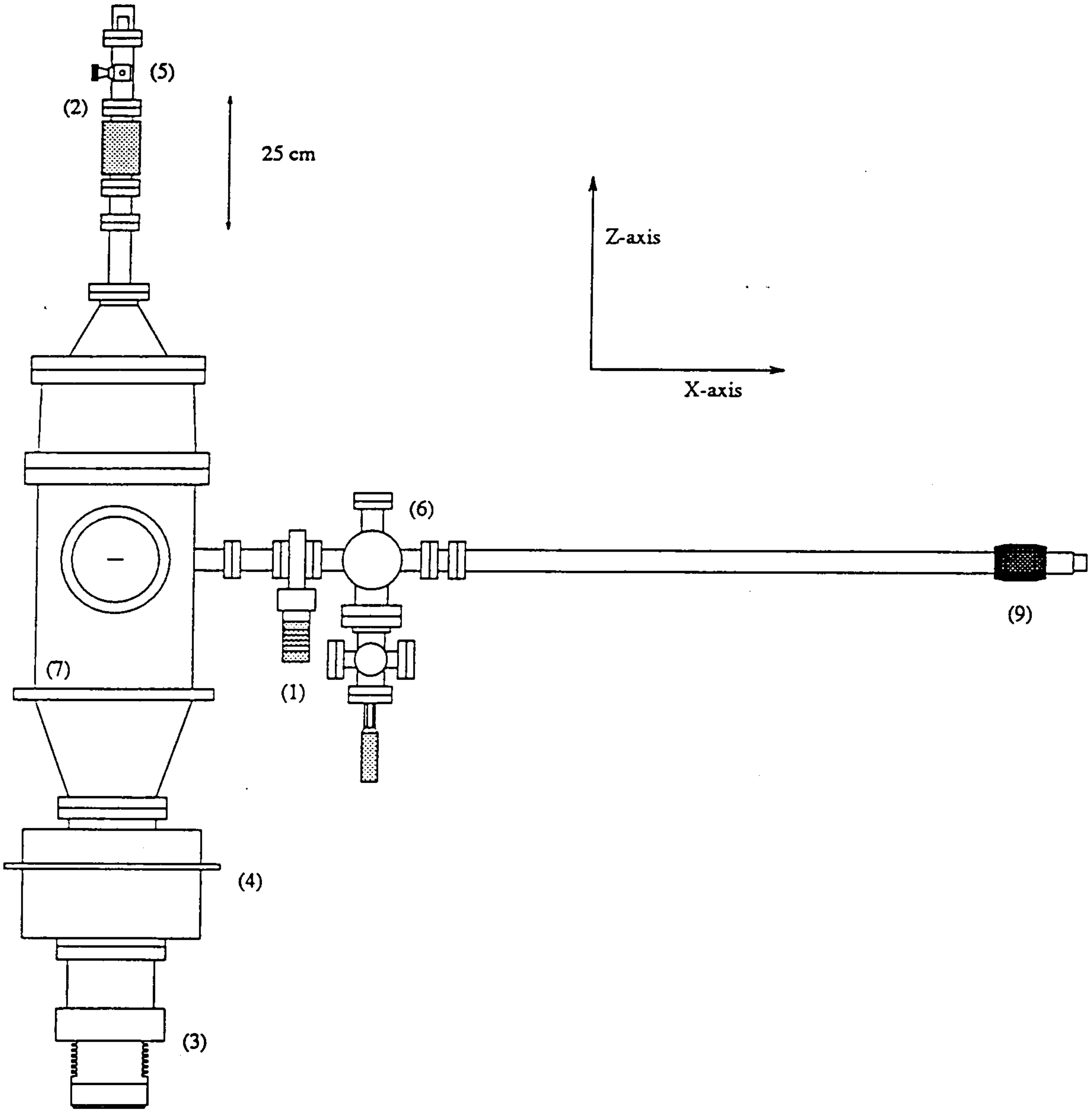

Figure 3.1 Schematic side view of the ERISS.

In figure 3.1 a schematic side view of the ERISS apparatus is shown. Numbers in braces refer to the numbers in figure 3.1. Ions are generated in the ion source (Leybold-Heraeus IQE-12/38) {2}. The ion source is differentially pumped by a 50 l/s turbo molecular pump

(Leybold-Heraeus turbovac 50). A high resistance aperture enables ions from the ion source to pass through the analyzer into the main chamber {7}. The main chamber has a base pressure of $1 \cdot 10^{-10}$ mbar and is pumped by a 300 l/s turbo molecular pump (Balzers TPH450H) {3} and a Ti-sublimation pump (Leybold-Heraeus V150-2) surrounded by liquid nitrogen cooled cryogenic panels {4}. Samples are inserted into the vacuum system through the separately pumped preparation and loading chamber {6}. The preparation and loading chamber is equipped with an oven to heat a sample and with a gas inlet for pretreatment purposes. The chamber is connected to the main chamber by a manually operated valve {1}. By using the magnetic transfer rod {9} samples can be loaded in the main chamber without breaking vacuum. Samples are placed in the manipulator, perpendicular to the drawing in figure 3.1. The manipulator can move the sample with respect to the ion beam in three perpendicular directions (x,y and z, as defined in the figure) and also rotate along the y-axis as defined in figure 3.1. Each of the five available places on the manipulator has a resistive spiral for heating the sample. In addition the manipulator is equipped with a Beam Profile Analyzer [7] to optimize the beam current and shape.

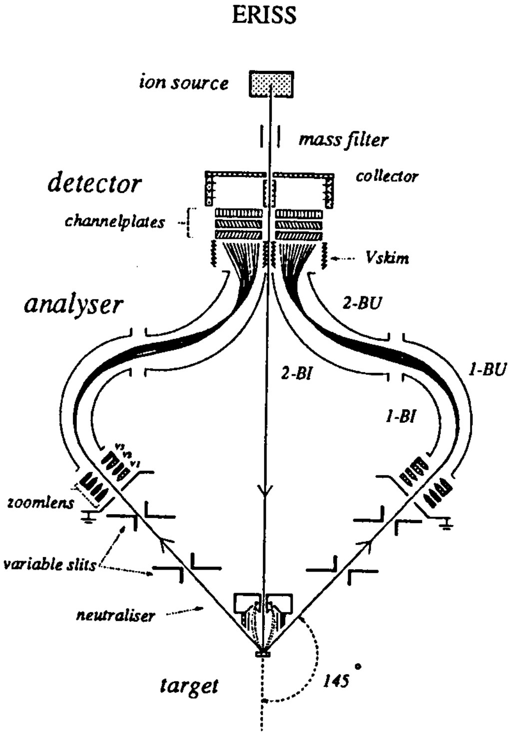

Figure 3.2 Schematic cross section of the ERISS analyzer and detector with ion trajectories.

The double toroidal electrostatic analyzer, used for analyzing the energy of the scattered ions, the detector and ion trajectories are depicted in figure 3.2. Ions from the ion source pass through the center of the detector and analyzer onto the sample. Ions scattered over 145° are accepted by the slits and are accelerated (V_3 in zoom lens, see figure 3.2) towards the analyzer. Besides defining the scattering angle, the slits can be adjusted to vary the solid angle of acceptance. Increasing the solid angle of acceptance increases the number of ions collected, but decreases the energy resolution and vice versa. The energy of ions which follow the central path of the analyzer is called the pass energy, E_{pass}. The pass energy depends only on the voltage applied to the separate electrodes of the analyzer. Ions with a kinetic energy in the range from (E_{pass}-5%) to (E_{pass}+5%) pass through the analyzer and reach the detector at a radius according to their energy relative to the pass energy of the analyzer. This means that for a typical pass energy of 3 keV the "energy window" is 300 eV. A complete energy spectrum is built up from smaller spectra taken at different acceleration potentials, while the pass energy is kept constant.

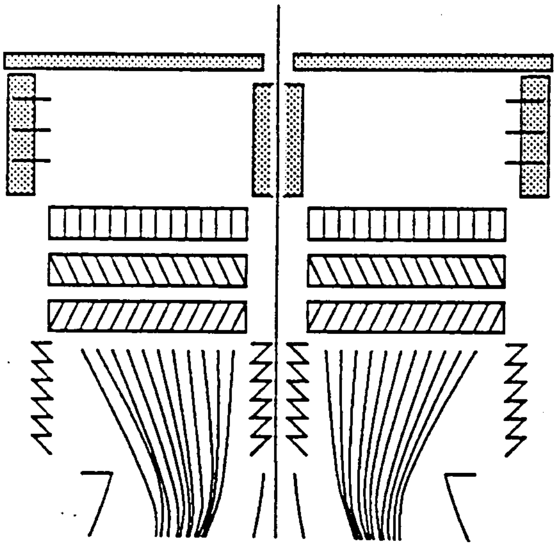

***Figure 3.3** ERISS detector with incoming ions, microchannel plates (MCP), drift space and collector.*

The detector (figure 3.3) consists of three multichannel plates (MCP), a drift space and the collector. An incident ion causes a cascade of electrons in the multichannel plates which results in a cloud of approximately 10^6 electrons, while the position of the incident ion is conserved. The electron cloud expands in the drift space due to coulomb repulsion to a size of approximately 2 mm in diameter and hits the collector.

The collector is a modified wedge and strip collector (figure 3.4). The fraction of the total charge collected on the strips is a measure for the radius and thus for the energy of the ion that hit the first MCP, similarly the fraction of the total charge collected on the wedges is

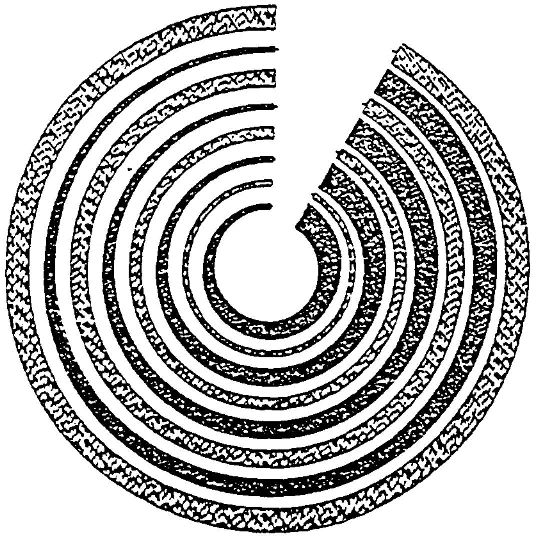

Figure 3.4 Schematic representation of the ERISS collector with 4 of the 14 wedge and strip sets. In the real collector the whist space in this figure is conducting and connected to ground.

a measure for the azimuth where the ion hit the first MCP. To prevent charging of insulating materials a neutralizer is available to spray electrons to the sample. This neutralizer is basically a heated ring-shaped filament around the ion beam with an anode at a typical voltage of 15 V, pulling the electrons out of it. A deflection plate directs the electron towards the sample. These electrons reach not only the spot on the sample where the beam incides but the whole sample. Electrons reach the sample from all directions and thus reach the whole surface even when it is not flat. The neutralizer current is typically a factor ten higher than the ion beam current.

To minimize damage to the surface during measurements the ion dose must be kept extremely low. This can be done by scanning the manipulator under the beam during measurements. In this way the effective beam spot can be increased from 0.3 mm^2, the typical cross-section of a focused ion beam, to a square of 5x5 mm^2 maximum. For the effective dose this means an enormous decrease and makes it possible to obtain spectra with ion doses less than 10^{12} ions/cm^2 using a beam current of typically 1 nA. The measurement of a spectrum of one "energy window" takes typically 30 seconds.

The ion beam is also used for sputtering and cleaning of samples. For this ion currents of up to 250 nA are used. Also the deflection plates of the Beam Profile Analyzer are used to scan the ion beam over a the sample.

3.2 Cleaning and pretreatment of samples.

Alloys and calibration samples.

Two Pd-Pt alloys were produced at Philips NatLab, one with 80 at% Pd and 20 at% Pt and the other with 20 at% Pd and 80 at% Pt. Both alloys were etched in an acidic mixture of 3 parts HNO_3 (60%) and 1 part HCl (36%), following the cleaning procedure described in the *CRC Handbook of Metal Etchants* [8]. After gas formation in the acid ceased, the alloys were washed in ethyl-alcohol. Then the alloys were polished using alumina powder with grain sizes of 50 micron down to 0.5 micron. Finally they were mounted and inserted in the vacuum system where several cycles of sputtering with a 250 nA, 3keV Ne^+ ion beam scanned over 5x5 mm for several hours and annealing at 400°C were carried out to remove any remaining contaminants.

Catalysts.

Pd/Pt catalysts were produced at KSLA by impregnation of an Al_2O_3 powder with Pt and Pd tetramine complexes followed by calcination at 300°C in air. One of these catalysts has 0.7 wt% Pd and 0.3 wt% Pt resulting in a bulk composition of $Pd_{20}Pt_{80}$, the other has 1.3 wt% Pd and 0.2 wt% Pt resulting in a $Pd_{80}Pt_{20}$ bulk composition. To minimize inhomogeneities and to increase the density the grains were powdered in a mortar and pressed with a load of 1600 kg in a tantalum cup.

Pretreatments.

To investigate changes in the surface composition in different chemical environments both the alloys and the catalysts received a pretreatment. This was done in the pretreatment chamber, connected to the main chamber. This, to avoid contamination during transportation after pretreatment. First, the sample was inserted in the oven and the chamber was filled with either hydrogen or oxygen at a pressure of 500 mbar. The temperature of the oven is monitored by a thermocouple mounted to it. During filling the chamber with gas or pumping gas out of the chamber, the oven is always turned off to prevent electrical breakthrough. Depending on the pretreatment, the oven temperature control was set to 350°C or not turned on. In order to simulate flow conditions the gas was refreshed after 15 minutes. Another 15 minutes later the oven control was turned off again and the gas was evacuated while the sample cooled down. When the pressure in the pretreatment chamber was below 10^{-6} mbar and the sample was cooled, the sample was transported to the manipulator in the main chamber.

4. Results and discussion.

4.1 Static LEIS.

To be sure the results on fragile surfaces such as catalysts are reliable, it has been investigated that these results are indeed obtained under static conditions, i.e. only negligible damage to the surface occurs upon ion bombardment during measurements. In figure 4.1 two successive spectra of a $Pd_{80}Pt_{20}/Al_2O_3$ catalyst covered with H_2 are shown. The ion dose used for these measurements is $1.2 \cdot 10^{13}$ ions/cm^2, with an ion current of 1 nA. Since there are in the order of 10^{15} atoms/cm^2 on the surface, an ion dose as used here means that approximately 1% of the surface atoms has taken part in a scattering event. From the given spectra it is clear that the difference in the measured peak areas is negligible and therefore the damage to the surface is also negligible. A small increase may be detected due to the partial sputtering of the adsorbed hydrogen. The typical sputter yield for hydrogen adsorbed on Pd is 10.9 atoms/ion and 12.5 for hydrogen adsorbed on Pt for Ne^+ ions [9]. Under these circumstances static LEIS is guaranteed.

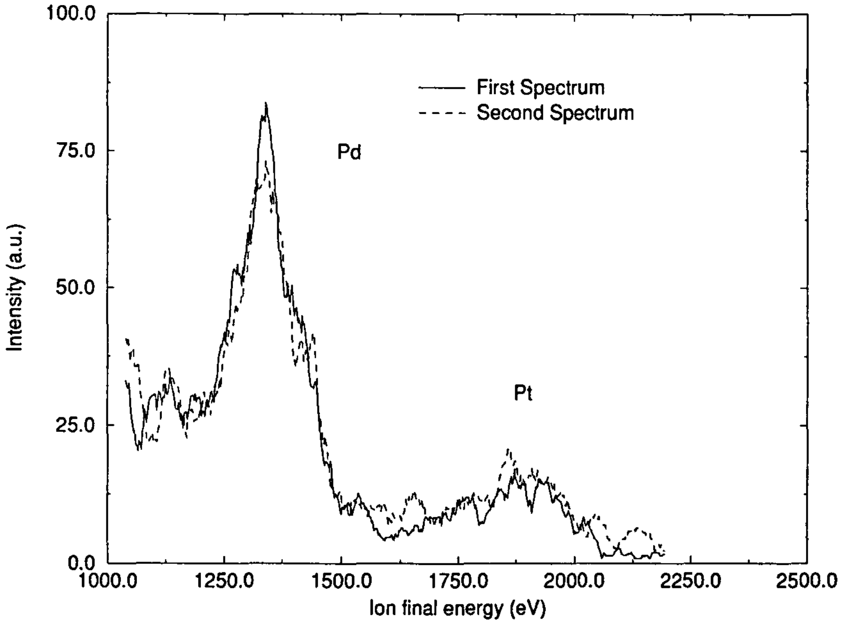

Figure 4.1 *Two successive spectra of Pt and Pd of hydrogen adsorbed on a $Pd_{80}Pt_{20}/Al_2O_3$ catalyst using an ion dose of $1.2 \cdot 10^{13}$ ions/cm^2.*

Den Otter *et al.* **[10]** have performed molecular dynamics simulations of ion scattering on small Rh clusters of 147 atoms. They found that in some events only one ion could deposit enough energy in a cluster causing it to explode. The probability of these events were not presented. However, this must be kept in mind when LEIS is performed on small metal clusters.

4.2 Pure elements.

To obtain information on the concentration of the elements on the surface all measured peak intensities have to be compared to the peak intensities of the pure elements. In figure 4.2 the spectra obtained from scattering 3keV Ne^+ on poly-crystalline Pd and Pt samples are given. The intensities have been normalized to the current of the ion beam. As can be seen the sensitivity for both platinum and palladium is almost equal, taking into account the surface density of the pure elements. The surface density, calculated by taking the bulk density to the power 2/3, is $1.66 \cdot 10^{15}$ atoms/cm^2 for Pd and $1.64 \cdot 10^{15}$ atoms/cm^2 for Pt. With a ratio of the areas under the palladium peak and under the platinum peak of 1.03, the sensitivity of palladium is 1.01, relative to the sensitivity of platinum. The error in determining a peak area is at least 1%. Therefore the relative sensitivities of Pd and Pd are considered equal from here on.

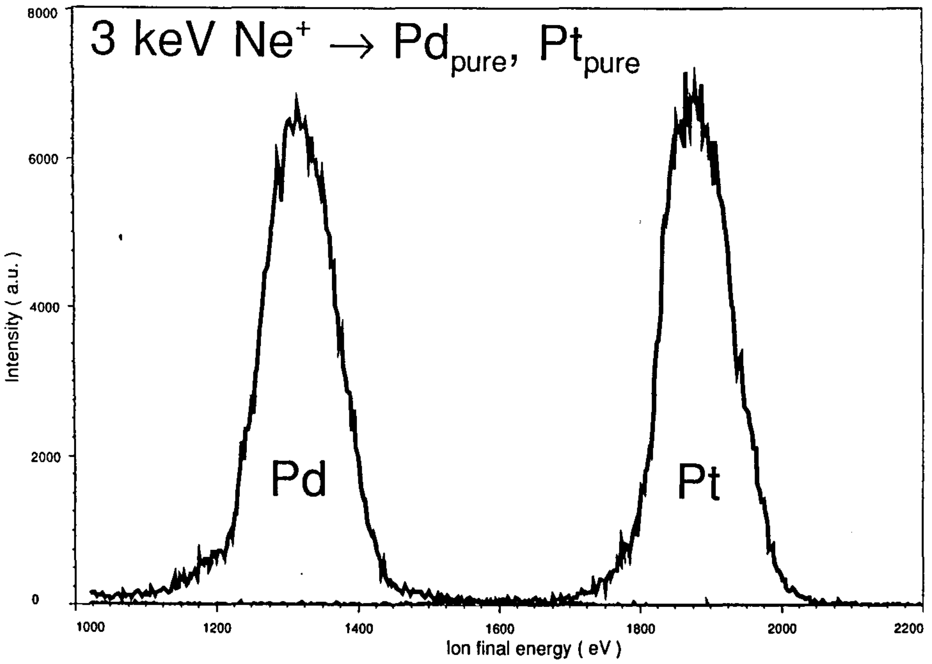

***Figure 4.2** LEIS spectra of the pure samples of (a) platinum and (b) palladium using a 3keV Ne^+ ion beam. The spectra are normalized to an ion beam current of 1 nA.*

4.3 Alloys.

The segregation processes in supported small bimetallic clusters may differ from those in bulk alloys. To study segregation processes in these clusters, a comparison to bulk alloys must be made. On both systems treatments in O_2 and H_2 were done. However, this work will mainly concentrate on the influence of H_2 on the segregation processes

All measurements on the alloys were performed with a beam current of 200 pA during 70 seconds while the target was scanned under the beam over an area of 0.11 cm^2. This results in an ion dose of 8.10^{11} ions/cm^2. Sputtering between measurements was done with beam currents ranging from 200 pA up to 200 nA. During sputtering, the beam was scanned over the target using the deflection plates of the Beam Profile Analyzer. The sputtered area was 0.2 cm^2, slightly larger than the measuring area to prevent boundary effects. Since both the surface density and the sensitivity for Pd and Pt are about equal, the surface concentration of Pt can be defined as the ratio of $S_{Pt}/(S_{Pt}+S_{Pd})$, where S_i (i=Pt or Pd) is the signal of component i, normalized to the ion beam current.

The alloys were sputtered until no change in both the Pt and the Pd signal was observed. Furthermore, it was checked that no other elements were present at the surface. This is done by calculating the absolute coverage of both the Pd and the Pt, by normalizing both metal signals to the metal signals from the pure elements and ion beam current. When no other elements are present, the absolute coverages of Pt and Pd added is equal to 1 ML.

Hydrogen adsorbed on a surface is known to cause a large decrease in signal from the surface. The physical shielding of the hydrogen atom is too small to account for the decrease when Ne^+ ions are used. This leaves only the possibility that hydrogen adsorbed on the surface causes an increase of the neutralization probability [9] of the incoming or outgoing ions. Therefore it must be investigated if this influence is equal for both platinum and palladium. This is done by first applying hydrogen on an alloy and monitoring the ratio of platinum and palladium as the hydrogen is sputtered from the alloy. In figure 4.3 the normalized peak area of platina is plotted against the normalized peak area of palladium for two different Pd-Pt alloys. In this plot it is clear that the ratio of platina and palladium remains constant. The ratio differs from the bulk ratio due to sputtering. From this it can be concluded that the influence of hydrogen shielding is equal for both platinum and palladium. Because for *both* the alloys the ratio of platinum over palladium stays constant over the whole range of hydrogen coverages, the sputter yields of hydrogen adsorbed on platinum and of hydrogen adsorbed on palladium must be equal. Bergmans [9] has found sputter yields of 12.5 atoms/ion for hydrogen on platinum and 10.9 for

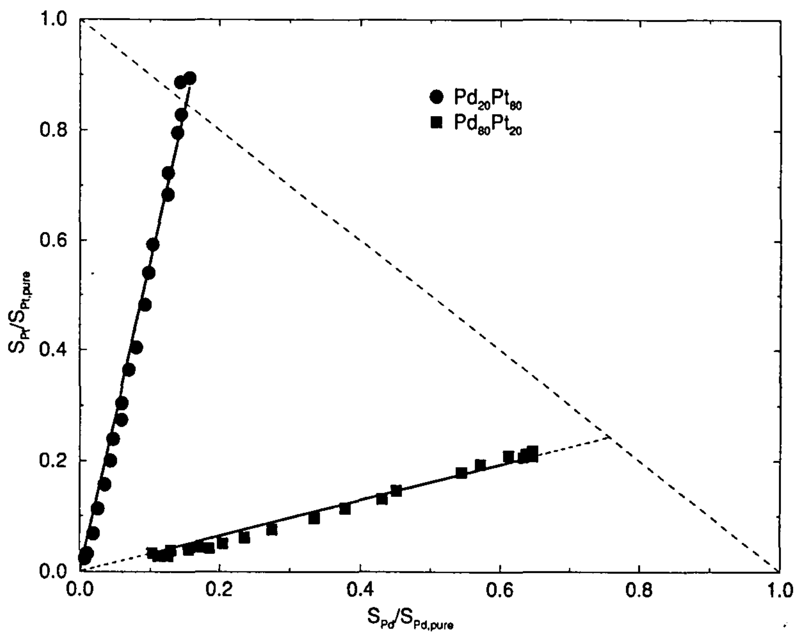

***Figure 4.3** The influence of hydrogen on Pt and Pd LEIS signals for a $Pd_{20}Pt_{80}$ and a $Pd_{80}Pt_{20}$ alloy.*

hydrogen on palladium (equal within the accuracy) when Ne^+ ions are used, cf. sputter yields of 2.0 atoms/ion and 1.4 atoms/ion for Pd and Pt respectively [12].

In figure 4.4 the surface composition of $Pd_{20}Pt_{80}$ is shown for the different pretreatments and the change of it on sputtering, in figure 4.5 the same is shown for $Pd_{80}Pt_{20}$. For all treatments it can be seen that the measured surface platinum content changes to 85% for the $Pd_{20}Pt_{80}$ alloy and to 26% for the $Pd_{80}Pt_{20}$ alloy. This can be understood from the different sputter yields of platinum and palladium, respectively.

At sufficiently low temperatures, where bulk diffusion can be neglected, a simple relation can be given between sputtering yields and surface concentrations. For a binary target the derivation is as follows [11].

At sputter equilibrium the ratio of the number of sputtered atoms n_A of component A to n_B of component B is equal to the ratio of the bulk concentrations :

$$n_A/n_B = c_A/c_B.$$

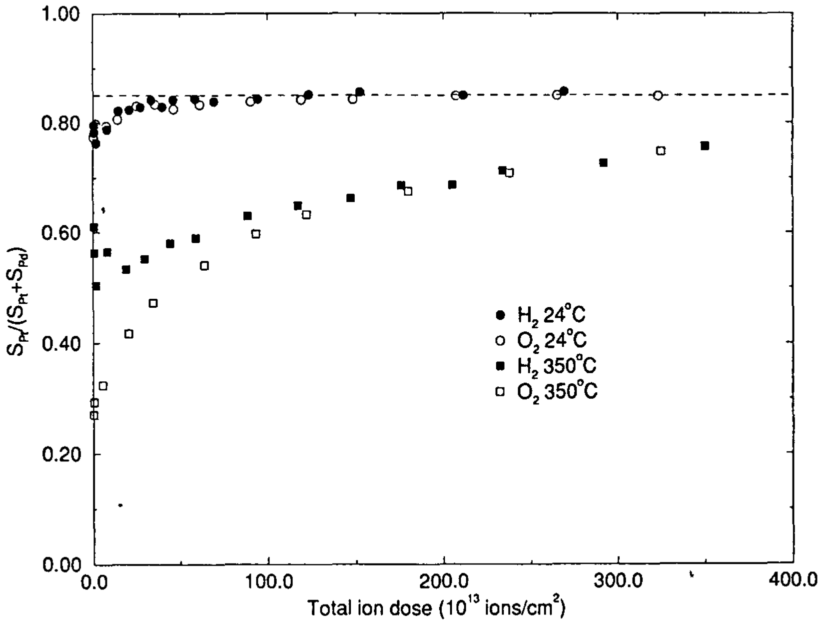

***Figure 4.4** Development of $S_{Pt}/(S_{Pt}+S_{Pd})$ as a function of the total ion dose applied for the $Pd_{20}Pt_{80}$ alloy.*

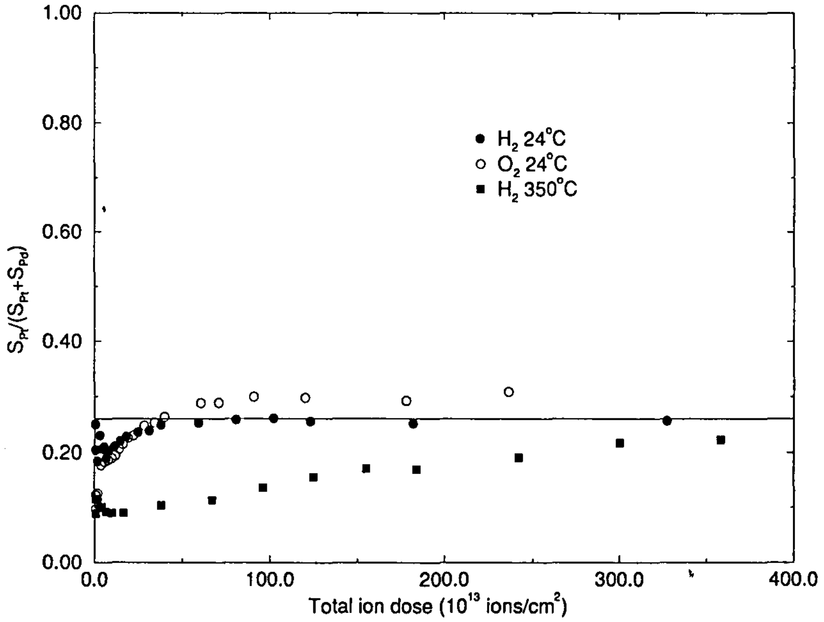

***Figure 4.5** Development of $S_{Pt}/(S_{Pt}+S_{Pd})$ as a function of the total ion dose applied for the $Pd_{80}Pt_{20}$ alloy.*

The ratio of the number of sputtered atoms n_A/n_B is equal to the ratio of the partial sputtering yields Y_A/Y_B (definition of the sputtering yield). From this the following relation for steady-state between the surface concentrations c^s_A/c^s_B and the bulk concentrations c_A/c_B can be found :

$$(c^s_A/c^s_B) = (c_A/c_B)/(Y_A/Y_B).$$

When this equation is applied to Pd and Pt with sputtering yields of 2.0 atoms/ion and 1.4 atoms/ion respectively [12], the ratio of the bulk concentrations is changed by a factor of 1.43 for the surface concentration. For the $Pd_{20}Pt_{80}$ alloy this results in a Pt concentration of 85% and for the $Pd_{80}Pt_{20}$ in 26%, at sputter equilibrium. This explains the deviation from the bulk composition. Du Plesis and Taglauer [13,14] reported no segregation after sputtering in Pt-Pd alloys at room teperature.

4.3.1 Room temperature pretreatment.

When oxygen or hydrogen is applied to one of the alloys at room temperature, it causes a decrease of the total metal yield of approximately 93%. The signal of the remaining 7% Pd and Pt on the surface gives a clearly distinguishable signal of both palladium and platinum, as can be seen in figure 2.1. 83% of this remaining metal signal is platinum when oxygen is applied and 77% when hydrogen is applied. While sputtering the oxygen from the surface, the platinum concentration increases to 85% after a total ion dose of $5\cdot10^{14}$ ions/cm^2. This is the expected sputtered surface composition as started with before pretreatment. A similar effect is seen on the $Pd_{80}Pt_{20}$, where the platinum concentration directly after pretreatment is equal to 20%.

From these results it can be concluded that oxygen and hydrogen pretreatment at room temperature have no major influence on the surface composition of this alloy, apart from the shielding by the adsorbates. Thermodynamics predict a palladium enrichment at the surface due to the lower surface energy of palladium (γ_{Pt}=243 10^{-6}J/cm^2, γ_{Pd}=198 10^{-6}J/cm^2) [15]. However, this is not observed since the surface is not in thermodynamic equilibrium because of the previous sputtering. The mobility for segregation get significantly important only for temperatures in the order of or higher than about 1/3 of the melting temperature [16]. Therefore no segregation is expected at room temperature after sputtering, as observed by du Plesis and Taglauer [13,14]. Figure 4.6 shows the platinum signal versus the palladium signal for both alloys after room temperature pretreatment with oxygen. The results for the pretreatment with hydrogen were already given in figure 4.3. As can be seen in figure 4.6, the ratio of the platinum signal and the palladium signal is constant for both the alloys and for the whole coverage range of oxygen. One can conclude that, as for the adsorbed hydrogen, the sputtering yields of oxygen adsorbed on platinum and of oxygen adsorbed on palladium are not very different. Since the heat of adsorption of O_2 adsorbed on poly- crystalline Pd or Pt are almost equal ($\Delta H_{ads} \approx -70$ kcal/mol) [17] this seems reasonable.

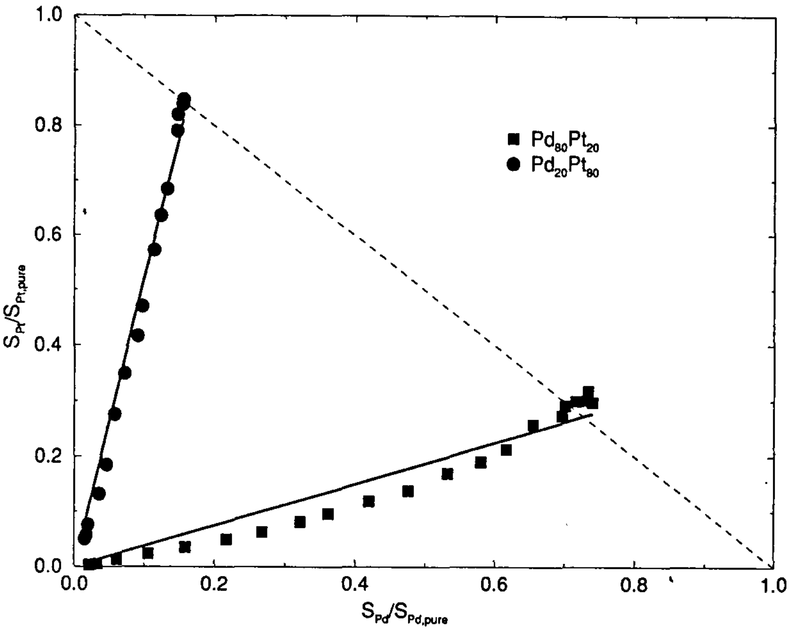

Figure 4.6 Detected amount of platinum vs. palladium upon sputtering after pretreatment with O_2 at room temperature for both the $Pd_{20}Pt_{80}$ and the $Pd_{80}Pt_{20}$ alloy.

Summary of the change in S_{Pt} / (S_{Pt} + S_{Pd}) after pretreatment of the $Pd_{20}Pt_{80}$ and the $Pd_{80}Pt_{20}$ alloy.

	Temperature : 24°C		Temperature : 350°C	
Alloy :	Oxygen	Hydrogen	Oxygen	Hydrogen
$Pd_{20}Pt_{80}$	83%	77%	28%	50%
$Pd_{80}Pt_{20}$	20%	20%		9%

4.3.2 Pretreatment at 350°C.

Oxygen and hydrogen pretreatment at 350°C causes a decrease of approximately 89% of the metal yield. This slightly lower decrease of metal signal compared to the decrease when oxygen is applied at room temperature, is probably due to desorption during evacuation after pretreatment when the sample was still hot. In figures 4.4 and 4.5 the development of $S_{Pt}/(S_{Pt}+S_{Pd})$ vs. the total ion dose is depicted. For oxygen pretreatment the platinum concentration is initially 28% for the $Pd_{20}Pt_{80}$ alloy. Hydrogen applied at 350°C shows a platinum concentration of 50% for the $Pd_{20}Pt_{80}$ alloy and 9% for the $Pd_{80}Pt_{20}$ alloy. It can be seen in figures 4.4 and 4.5 that the Pt/Pd ratio shifts gradually to the sputtering steady-state ratio.

For both the oxygen and the hydrogen applied at 350°C a palladium enrichment is observed. This is in accordance with thermodynamics which predict an enrichment in palladium at the surface due to the lower surface energy of palladium **[15]**. Experiments where the alloys were annealed to 350°C, without hydrogen or oxygen present, were not performed on these alloys.

Chemical induced segregation can not account for the palladium enrichment. The heats of adsorption of hydrogen on palladium or platinum are about equal (approx. 30 kcal/mol). The same is true for the heats of adsorption of oxygen on palladium or platinum (approx. 70 kcal/mol) **[17]**.

4.4 Catalysts.

Measurements on the catalysts were performed by scanning the sample under the ion beam over an area of 0.11 cm^2. Between measurements there was no additional sputtering as with the alloys, the measuring beam was used as sputter beam. Between measurements the ion beam current was increased to sputter more material from the surface. Measured yields were normalized to the current.

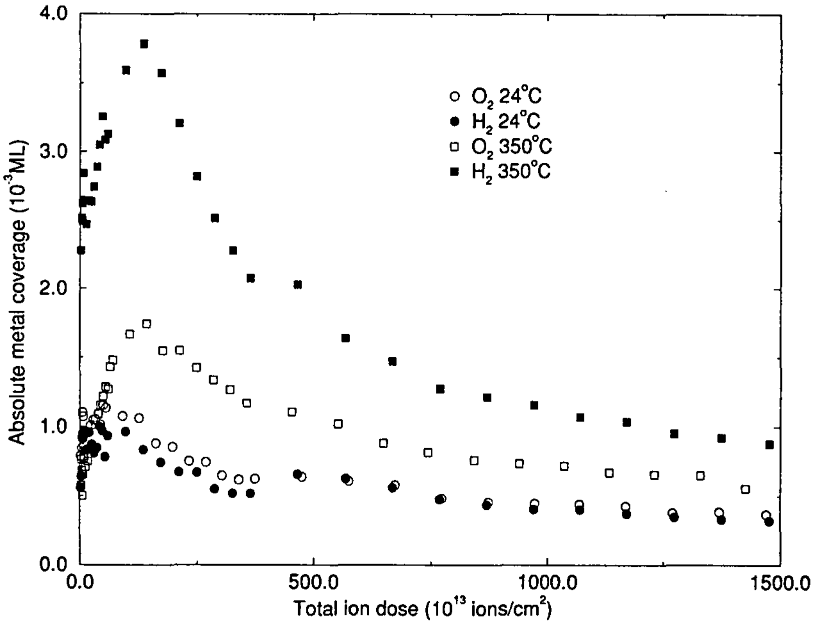

Figure 4.7 Development of the absolute metal coverage with increasing total ion dose for the $Pd_{20}Pt_{80}/Al_2O_3$ catalyst.

Figure 4.7 shows the total metal signal development with increasing incident ion dose in sputter experiments on the $Pd_{20}Pt_{80}/Al_2O_3$ catalyst. A rise in the combined signal of Pd and Pt is observed, followed by a decrease after a total ion dose of approximately $2 \cdot 10^{15}$ ions/cm^2. The origin of the initial rise is the removal of the adsorbed species and thus a larger exposure of the underlying metal clusters. Another contribution to this rise can be the destruction and subsequent spreading of clusters due to the ion beam. The decrease in signal can be explained by assuming that not all metal clusters are of the same size and thus the smallest clusters will be removed more rapid due to sputtering than the larger clusters. The removed clusters cause a decrease of the total metal yield. The signal does not completely vanish because new clusters are appearing for the ion beam after support material is sufficiently sputtered. From the normalized and combined metal signals, an estimate of the cluster size can be calculated :

The metal atom concentration (N_{met} [cm^{-2}]) can be calculated from the weight percentage of the metal (wt% [g/g]), the specific area of the catalyst (c [cm^2/g]) and the mass of the metal atom (M_{met} [amu]):

$$N_{met} = wt\% \,/\, (c \cdot M \cdot 1.66 \cdot 10^{-24})$$

Taking the values of wt% = 0.01, c = $2 \cdot 10^6$ cm^2/g, and the average mass of the atom $0.8 \cdot 106.4 + 0.2 \cdot 195.1$ (for the $Pd_{80}Pt_{20}$ system) this results in $2.4 \cdot 10^{13}$ metal atoms/cm^2.

The number of atoms visible to the ion beam (N^*) and the metal atom concentration are related by

$$N^* = \alpha \cdot N_{met}$$

where α is a shape dependent factor, for instance for a cubic cluster α is 1/d where d is the number of atoms on one edge of the cube. N^* can be calculated from the ion yield normalized to the ion yield from a pure sample and the surface density of the pure sample. An estimate of N^* is $1.6 \cdot 10^{12}$, when 0.1% of a monolayer is observed. Together with the calculated value of N_{met} this results in a value of 0.067 for α. Assuming a cubic cluster this means that the cluster size is 15 metal atoms, about 4 nm in diameter.

In figure 4.8 the development of $S_{Pt}/(S_{Pt}+S_{Pd})$ with increasing total ion dose is shown after the different pretreatments of the $Pd_{20}Pt_{80}/Al_2O_3$ catalyst. In figure 4.9 the development of $S_{Pt}/(S_{Pt}+S_{Pd})$ with increasing total ion dose after the different pretreatments of the $Pd_{20}Pt_{80}/Al_2O_3$ catalyst is shown.

4.4.1 Room temperature pretreatment.

When both $Pd_{20}Pt_{80}/Al_2O_3$ and $Pd_{80}Pt_{20}/Al_2O_3$ catalysts are pretreated with oxygen or hydrogen at 24°C, the observed platinum concentration is within the accuracy equal to the bulk concentration of the clusters. This can be explained by assuming that during the production the clusters have a homogeneous distribution of both platinum and palladium and that at room temperature the mobility of the atoms is too small for segregation. In addition to this, it should be noted that the last step in the production of the catalysts is a calcination in air at 300°C, which means that the clusters are oxidized and the surface energies are different from the metal surface energies.

The maximum metal yield observed is approximately 0.12% of the yield from a clean alloy. It can be concluded that as for the alloys, the pretreatment with oxygen and hydrogen at room temperature has no noticeable influence on the surface composition.

Summary of the change in S_{Pt} / (S_{Pt} + S_{Pd}) *after pretreatment of the* $Pd_{20}Pt_{80}/Al_2O_3$ *and the* $Pd_{80}Pt_{20}/Al_2O_3$ *catalysts.*

	Temperature : 24°C		Temperature : 350°C	
Catalyst :	Oxygen	Hydrogen	Oxygen	Hydrogen
$Pd_{20}Pt_{80}/Al_2O_3$	80%	80%	24%	100%
$Pd_{80}Pt_{20}/Al_2O_3$	30%	22%	40%	100%

4.4.2 Pretreatment at 350°C.

When the $Pd_{20}Pt_{80}/Al_2O_3$ catalyst is pretreated with oxygen the platinum surface concentration decreases to 20%, the same behaviour as seen on the $Pd_{20}Pt_{80}$ alloy. The maximum metal signal is a factor two higher than on the room temperature pretreated catalyst. For the $Pd_{80}Pt_{20}/Al_2O_3$ catalyst the platinum concentration is 40% initially and decreases to 17% after a total ion dose of $1 \cdot 10^{15}$ ions/cm^2. The most drastic changes are observed when hydrogen is applied to the catalysts at 350°C. The platinum concentration on $Pd_{20}Pt_{80}/Al_2O_3$ catalyst is 100%, so no palladium was found on the surface, in contradiction to the enrichment of palladium as observed on the alloy. After a total ion dose of $2 \cdot 10^{15}$ ions/cm^2 only 8% of the metal visible is palladium. This does not change at least up to an ion dose of $1 \cdot 10^{16}$ ion. For the $Pd_{80}Pt_{20}/Al_2O_3$ catalyst it is also seen that the outermost surface has a platinum concentration of 100%. After $3 \cdot 10^{15}$ ions/cm^2 the palladium concentration has increased to 32% to stay constant at least up to an ion dose of $1 \cdot 10^{16}$ ions/cm^2. Another effect is the increase of the maximum metal yield by a factor 4 to 0.43% of the yield from the corresponding alloy. This is an indication that the size of the clusters has increased or spread over the surface in comparison to the clusters on the catalyst treated at room temperature.

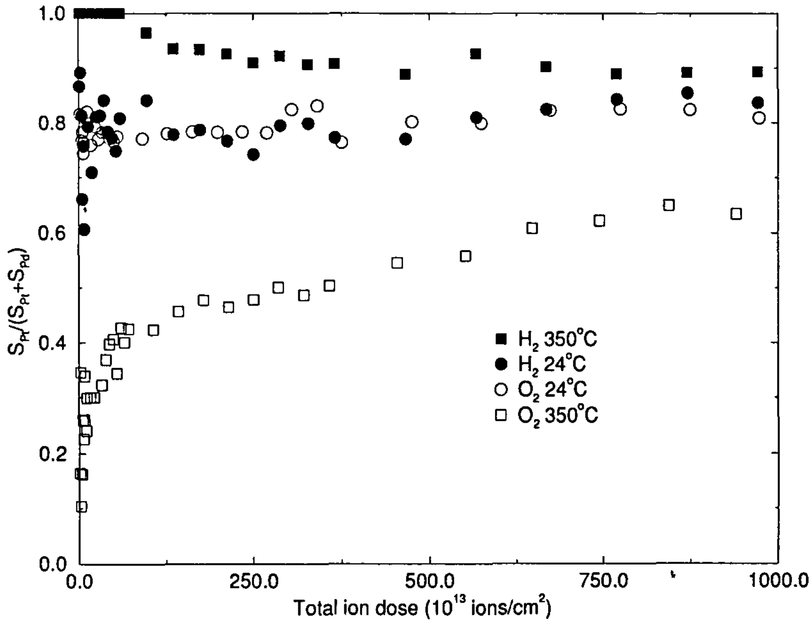

***Figure 4.8** Development of $S_{Pt}/(S_{Pt}+S_{Pd})$ as a function of the total ion dose applied for the $Pd_{20}Pt_{80}/Al_2O_3$ catalyst.*

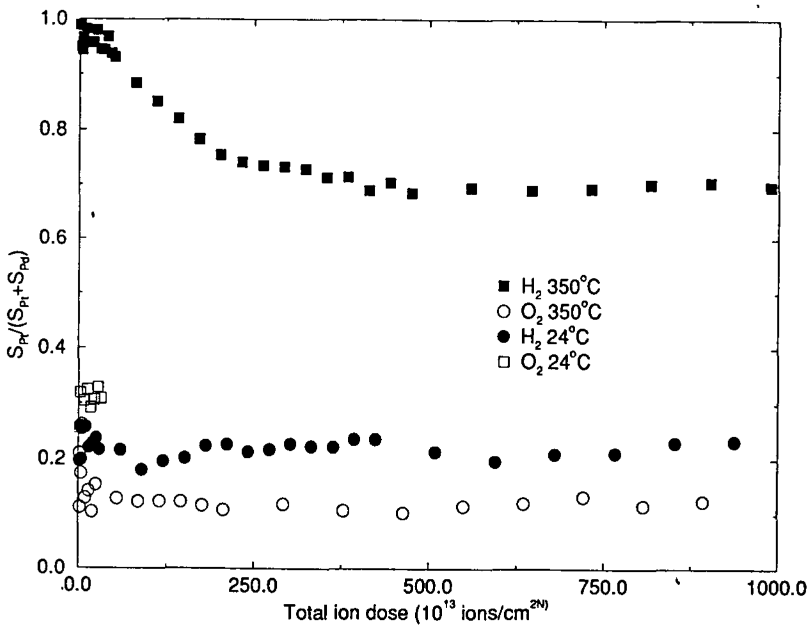

***Figure 4.9** Development of $S_{Pt}/(S_{Pt}+S_{Pd})$ as a function of the total ion dose applied for the $Pd_{80}Pt_{20}/Al_2O_3$ catalyst.*

Discussion.

The enrichment of platinum on the outermost surface layer of the clusters, after reduction with H_2 at 350°C, can be caused by chemical induced segregation, but that is very unlikely. The heats of adsorption of hydrogen on palladium or platinum are almost equal (see alloys), so there is no driving force for this chemical induced segregation.

The effects of segregation observed in the supported metal clusters is different from what is observed in the alloys. Therefore the segregation process in the metal clusters must be due to a segregation parameter which plays no part in possible segregation processes in alloys; the influence of cluster size and metal support interaction.

The small size of the clusters has two implications. The limited number of atoms in the clusters and the exposure of specific surface planes with a possible reconstruction induced by H_2. These planes do not necessarily have the same surface composition as the planes in poly-crystalline surfaces where a palladium enrichment is expected [15].

The other difference between alloys and supported bimetallic catalysts is interaction of the metal with the support, which is absent in the alloys. Tauster and Fung [19] suggest that for several reducible oxide supports a strong interaction with the supported metal exists. This is called the Strong Metal-Support Interaction, or SMSI. They also suggest that Al_2O_3 has no SMSI properties. Contrary to this, other authors report (strong) metal-support interaction for platinum clusters on an Al_2O_3 support [20]. Yao reviewed [21] several models to explain the loss of the H_2 adsorption capacity of Pt metal clusters on Al_2O_3 after reduction by H_2 at $\geq$ 500°C, compared to that at 300°C. Some of these are (1) the formation of a Pt_3Al alloy, (2) the formation of small thin box-like structures of Pt, (3) aggregation of Pt atoms in a two-dimensional phase into three-dimensional clusters, without affecting the size of the existing 3D clusters. These models will be included in the interpretation of our results.

The morphology of the clusters is influenced by these metal-support interactions. Spreading of the cluster can be induced by lowering the interface energy by reducing the support. Bulk reduction of Al_2O_3 is thermodynamically impossible at the temperatures used. The oxidic support can be reduced at the interface with the metal cluster as reported by Den Otter and Dautzenberg [22]; in the reduction of oxides of base metals it is seen that the temperature at which the reduction of the oxides starts can be decreased by several hundred degrees when small amounts of metals, able to desorb hydrogen dissociatively, are present on the surface. They also report platinum-aluminum alloy formation at the metal-support interface after reduction at 600°C.

With this in mind, a possible mechanism describing the processes during reduction in H_2 at 350°C qualitatively, can be formulated. First hydrogen adsorbs dissociatively on the metal cluster and migrates through the cluster towards the metal-support interface. The support at the interface will then be (partly) reduced. The modified support at the interface will be less compatible with the metal, due to a higher interface energy, and the clusters tend to break up into smaller clusters [20]. Alternatively, after reduction Pt-Al and/or Pd-Al alloys are formed which causes spreading of the cluster due to a lower metal-support interface energy. Both possibilities lead to an effective higher surface concentration of the Pd and Pt, as is shown by the increase of the total metal signal after pretreatment with H_2 at 350°C. In the case of preferential formation of palladium-aluminum alloys (when the Pd-Al bond is stronger than the Pt-Al bond) a migration of palladium atoms to the interface and thus away from the surface can be expected. This is in accordance with the observed platinum enrichment at the surface. However, no value for the metal-aluminum binding energy can be given because several PdAl and PtAl alloy compounds can exist and it is not known which alloys are formed at the interface. Using predicted values for the enthalpy of formation of e.g. PdAl and PtAl, -84 kJ/mol and -82 kJ/mol respectively [23], indicates a very small advantage for the PdAl.

The above mentioned models are previously reported in literature for Pt/Al_2O_3, but were applied for reduction at higher temperatures. Cairns *et al.* [20] reported agglomeration of a Pt layer on an alumina substrate into clusters at 1000°C and subsequent interdiffusion between elements from the reduced support and the metal. Den Otter and Dautzenberg describe the formation of an alloy from highly dispersed Pt clusters on Al_2O_3 at 500°C. The temperature used in this work is lower and thus the effect is not expected to be as drastic as described by the above mentioned authors.

Another feature of the clusters must be taken into account. After production the metal clusters are still oxidized. Room temperature reduction might not be sufficient to reduce the whole cluster. The metal signal of a (partial) oxidized cluster can be lower than that of a fully reduced cluster. Therefore, the conclusions of the room temperature reduction experiments must be regarded with great care.

5. Conclusions.

With the new ERISS apparatus it is possible to perform Low Energy Ion Scattering under static conditions, while the LEIS signals are still distinguishable from the background.
The influence on the neutralization probability of hydrogen adsorbed on palladium is equal to the influence of hydrogen adsorbed on platinum. This means that hydrogen adsorbed on Pd-Pt samples has no influence on the Pt/Pd ratio of the LEIS signals.
The sputter yield of hydrogen when adsorbed on palladium is equal to the sputter yield of hydrogen when adsorbed on platinum when 3keV Ne^+ ions are used. The sputter yields of oxygen is also the same when it is adsorbed on either palladium or platinum.
Annealing a $Pd_{20}Pt_{80}$ or $Pd_{80}Pt_{20}$ alloy in 500 mbar H_2 or O_2 to 350°C induces a palladium enrichment at the surface. It is not clear whether this is due to the annealing alone or to the combination of annealing and the presence of H_2 or O_2, although chemical induced segregation is not likely. Annealing to achieve thermal equilibrium, without H_2 or O_2 present, was not performed and is recommended to be performed for further research.
Room temperature pretreatment with 500 mbar H_2 or O_2 of $Pd_{20}Pt_{80}/Al_2O_3$ and $Pd_{80}Pt_{20}/Al_2O_3$ catalysts yields a surface composition equal to the bulk composition.
Pretreatment of the $Pd_{20}Pt_{80}/Al_2O_3$ and the $Pd_{80}Pt_{20}/Al_2O_3$ catalysts at 350°C with 500 mbar H_2 indicates a surface enrichment with platinum, contrary to the corresponding alloys. This can be explained by a model where dissociatively adsorbed hydrogen migrates to the cluster-support interface and reduces the support at the interface. The reduction of the support at the interface causes either spreading of the cluster or the break up of clusters into smaller clusters.

Recommendations for further research :

LEIS measurements should be performed on the fresh catalysts and on both the alloys and the catalysts annealed in the absence of H_2 or O_2. This to eliminate the influence of the gas.
A reduction of the catalysts should be performed before other pretreatments are performed, to be sure to start with fully metallic clusters.
XPS measurements on the catalysts should be done to check the formation of aluminum alloys at the metal-support interface.
To verify the break up of clusters, Electron Microscopy studies should be done on the catalysts

Acknowledgments.

In this section I would like to thank some people for the support I received during my study at the University of technology and especially during my graduation in the Surface and Interface Group.

First of all I would like to thank my direct coach Arnoud Denier van der Gon and Hidde Brongersma for giving me the opportunity to work in the Surface and Interface Group (FOG) and on the ERISS apparatus in particular. I thank Martin Creusen for delivering a wonderful apparatus and, of course, Rein Rumphorst, Gerard Wijers and Wijnand Dijkstra for keeping it operational. Furthermore I thank Bert Roosenbrand and Rob van Veen for their support from the Koninklijke/Shell Laboratory in Amsterdam (KSLA) and Leon van den Oetelaar, Rob Bergmans and Jean-Paul Jacobs and the rest of the FOG group for sharing their expertise with me.

Furthermore I thank:
* The members of PerpeTUE Mobilé for their support and understanding. Special thanks go to M^{2}ark Mietus for his construction of the Beam Profile Analyzer.
* All my colleagues of Eurocinema Eindhoven for making it possible to work and earn some extra hard needed funds in a fun way.
* Joost Smans and Perrine Peeters for their support and criticism.
* The people I lived with at the Kerkstraat 42D : Eric, Mieke, Pauline, Albert, Ilse and Frank.

Finally I thank my parents, Joke and Will Nooij, and my brother Olivier Nooij and Marina Perry for being there when I needed them.

Oscar W. Nooij.
Eindhoven, 17 may 1995.

References.

[1] J.H. Sinfelt, *Bimetallic catalysts: discoveries, concepts and applications*, Exxon Monograph, John Wiley & Sons, New York (1983).

[2] S.M. Kovach and G.D. Wilson, United States Patent 3,943,053 (Mar. 9, 1976).

[3] A. G. Sault, Catal. Let. 29 (1994) 145.

[4] M. Creusen, Master Thesis, TUE 1994.

[5] H.H. Brongersma, F. Meyer and H.W. Werner, Philips Techn. Rev. T34 (1974) 367; H.H. Brongersma, M.Y. Sparnaay and T.M. Buck, Surf. Sci. 71 (1978) 657.

[7] M. Mietus, *Design, construction and implementation of a beam profile analyser for low energy ion beams*, IVO-TUE, 1994.

[8] *CRC Handbook of Metal Etchants*, Ed. P. Walker and W.H. Tarn, CRC Press, Boca Raton, Ann Arbor, Boston.

[9] R.H. Bergmans, PhD Thesis, (1995) to be published.

[10] W.K. den Otter, H.H. Brongersma and H. Feil, Surf. Sci. 306 (1994) 215.

[11] H.H. Anderson and H.L. Bay, in *Sputtering by Particle Bombardment*, vol. I, Ed. R. Behrish, Springer, New York, 1981.

[12] N. Matsunami, Y. Yamamura, Y. Itikawa, N. Itoh, Y. Kazumata, S. Miyagawa, K. Morita, R. Shimizu and H. Tawara, At. Data and Nucl. Data Tables, 31 (1984) 1.

[13] J. du Plesis and E. Taglauer, Surf. Interface Anal. 22 (1994) 556.

[14] J. du Plesis, G.N. van Wyk and E. Taglauer, Surf. Sci. 220 (1989) 381.

[15] F.J. Kuijers, B.M. Tieman and V. Ponec, Surf. Sci. 75 (1978) 657.

[16] H.H. Brongersma, private communications.

[17] I. Toyoshima and G.A. Somorjai, Catal. Rev. Sci. Eng. 19 (1979) 105.

[18] M. Vanhommerig, Master Thesis, TUE 1994.

[19] S.J. Tauster and S.C. Fung, J. Catal. 55 (1978) 29.

[20] J.A. Cairns, J.E.E. Baglin, G.J. Clark and J.F. Ziegler, J. Catal. 83 (1983) 301.

[21] H.C. Yao, Appl. of Surf. Sci 19 (1984) 398.

[22] G.J. den Otter and F.M. Dautzenberg, J. Catal. 53 (1978) 116.

[23] F.R. de Boer, R. Boom, W.C.M. Mattens, A.R. Miedema and A.K. Niessen, in *Cohesion and Structure*, vol I, Ed. F.R. de boer and D.G. Pettifor, North-Holland, Amsterdam, 1988.

Appendix.

Data on metals

Pd	Pt	Property
46	78	Atom number
106.4	195.1	Mass [amu]
12.0	21.5	Bulk density [kg/dm^3]
$1.66 \cdot 10^{15}$	$1.64 \cdot 10^{15}$	Surface density [atoms/cm^2]
1.01	1.00	Relative sensitivity (3keV Ne$^+$, ERISS)
2.0	1.4	Sputter yield (3keV Ne)
1820	2045	Melting temperature [K]
138	138	Atom radius [10^{-12} m]
70	70	$-\Delta H_{ads}$ of O_2 [kcal/mol] (estimate)
30	30	$-\Delta H_{ads}$ of H_2 [kcal/mol] (estimate)